

2016

**Phenomenological vs. mechanistic approaches for predicting species'  
responses to climate change**

Benjamin Martin, Andrew Pike, Sara John, Natnael Hamda, Jason Roberts, Eric Danner

## **ABSTRACT**

Predicting species responses to climate change is a central challenge in ecology, with most efforts relying on lab derived phenomenological relationships between temperature and fitness metrics. We tested one of these models using the embryonic stage of a Chinook salmon population. We parameterized the model with laboratory data, applied it to predict survival in the field, and found that it significantly underestimated field-derived estimates of thermal mortality. We used a simple biophysical model based on mass-transfer theory to show that the discrepancy was due to the differences in water flow velocities between the lab and the field. This mechanistic approach provides testable predictions for how the thermal tolerance of embryos depends on egg size and flow velocity of the surrounding water. We found strong support for these predictions across more than 180 fish species, suggesting that flow and temperature mediated oxygen limitation is a general mechanism underlying the thermal tolerance of embryos. We conclude that descriptive models of thermal tolerance can drastically underestimate species responses to climate change and that simple mechanistic models can explain substantial variation in the thermal tolerance of species.

## INTRODUCTION

Predicting how species will respond to the world's increasing air, ocean, and freshwater temperatures is a central challenge for ecology. A typical approach is to apply thermal performance curves (Angilleta 2006; Schulte et al 2011) that describe the relationship between some metric of fitness (mortality rate, growth rate, etc.) and temperature. These relationships, typically derived from laboratory data, are used to forecast species' responses to future temperature regimes in nature. As phenomenological models of thermal stress, these curves are not tied to any particular mechanism, and as a result are flexible tools that can be used to model any species or fitness metric. However, this flexibility comes with a cost: without a mechanistic understanding of underlying causes of thermal tolerance, the range of applicable conditions is not known. If the mechanism underlying thermal tolerance operates independently of other factors, for example by temperature-dependent protein denaturation (Fields 2001), then lab-derived models of thermal tolerance may be useful predictors in the field. However, other mechanisms of thermal sensitivity, such as oxygen-limitation (Pörtner 2007), depend not only on temperature, but also on other environmental and physiological variables that influence the demand or supply of oxygen to developing tissues. In such cases, thermal response forecasts that have been parameterized using laboratory response curves may be poor predictors of species responses in the field.

Here, we test whether such phenomenological approaches can predict the impacts of elevated water temperatures on endangered Sacramento River winter run Chinook salmon in the Central Valley of California. Since the construction of large dams on the Sacramento River in the mid-1900's, winter run Chinook have been blocked from reaching their native spawning grounds in cold, spring-fed mountain tributaries, and are now forced to spawn in the low-elevation

mainstem river below the lowest dam. In this new location, the thermal quality of their habitat is controlled by water releases from the dams. Because Chinook embryos are the most sensitive life-stage to elevated temperatures (McCullough 1999), a set of temperature related regulations governing dam operations were established to protect endangered winter run salmon eggs (NMFS 2008). Importantly, these regulations are based on thermal tolerance estimates from controlled laboratory experiments.

Here, we fit a phenomenological model of thermal tolerance to laboratory data on survival as a function of temperature and test whether it can retrospectively predict inter-annual variation in salmon survival through the embryonic stage in the Sacramento River. Although the phenomenological model successfully explained temperature-dependent survival in the lab, the model failed entirely at predicting the effects of temperature on survival in the field. We show that this is due to a  $\sim 3^{\circ}\text{C}$  reduction in thermal tolerance in the field compared to the lab. By applying a model based on mass-transfer theory to developing embryos, we show that oxygen limitation accounts for the observed discrepancy. Although mass-transfer theory is based on first-principles, and requires only a few easily measured parameters, it has not been extensively applied to predict the thermal tolerance of developing embryos. We show that mass-transfer theory can account for the discrepancy in thermal tolerance of Chinook embryos between lab and field contexts due to flow-dependent boundary layer effects. Furthermore we show how mass-transfer theory explains broad patterns of thermal tolerance across  $\sim 180$  oviparous fish species.

## **METHODS**

### ***Temperature-dependent mortality model***

We developed a phenomenological temperature-dependent survival model for Chinook embryos and fit the model to laboratory data. The temperature-dependent component of survival is determined by two parameters,  $T_{crit}$ , the temperature below which there is no mortality due to

temperature, and  $b_T$ , the slope at which instantaneous mortality rate increases with temperature above  $T_{crit}$ :

$$h_i = b_T \max(T_i - T_{crit}, 0) \quad \text{eq.1}$$

where  $T_i$  is the mean daily temperature experienced by a given embryo on the  $i$ th day of its development.

The survival probability during the  $i$ th day of development is:

$$s_i = \exp(-h_i) \quad \text{eq.2}$$

The model includes a temperature-dependent development rate (Zueg et al. 2009), where the number of days from fertilization to emergence was calculated based on the rate of development in day  $i$  is given by:

$$D_{i+1} = D_i + (0.001044 \times T_i + 0.00056) \quad \text{eq.3}$$

At fertilization  $D=0$ , and Chinook emerge on the day that  $D$  exceeds 1.

Egg survival throughout the entire embryonic period is given by the product of the daily temperature dependent survival probabilities from hatching to emergence, multiplied by the temperature-independent survival probability,  $\mu$ .

$$S = \mu \prod_{i=1}^n s_i \quad \text{eq.3}$$

We fit the model to embryonic survival data as a function of temperature compiled in Myrick and Cech (1999). We only included data for temperatures above 9°C because our model only considers mortality due to elevated (not low) temperatures and because winter-run Chinook embryos never experience water temperatures lower than 9°C in the Sacramento River.

### ***Application to the field***

We tested the ability of the laboratory-parameterized thermal tolerance model to predict inter-annual variation in egg-to-fry survival of winter run Chinook in the Sacramento River from 1996-2015. We linked existing datasets on the date and location of spawning with a 1-dimensional temperature model of the Sacramento River (Pike et al. 2012), with 1km spatial resolution, to generate daily temperature exposure profiles for all known redds (gravel spawning nests that salmon build) within years. We applied the survival model with lab-derived thermal tolerance parameters to the daily temperature exposure profiles for all known redds from 1996-2015. For each year we calculated the fractional population loss due to temperature-dependent mortality by aggregating the survival of all redds within that year. For all other sources of mortality in the field we included a temperature-independent background survival rate,  $\mu$ , which we treated as a free parameter. Additionally, in the field we hypothesized that, due to limited optimal habitat for spawning, mean redd quality decreases with increasing female spawner density. Thus we evaluated whether female spawner density affected ETF survival by evaluating a model including a density dependence term in the background survival rate:

$$\mu = \mu_0 + \mu_1 N \text{ eq.4}$$

### ***Parameter estimation***

We estimated model parameters for both the lab and field data sets via non-linear least squares. We searched parameter space for the parameter set that minimized the squared deviation between model predicted and observed survival. For the lab model, we used survival data as a function of temperature from the data sources reported in Myrick and Chech (2001). In the field we used winter-run egg-to-fry (ETF) survival to Red Bluff Diversion Dam estimated from USFWS from 1996-2015. We logit transformed the dependent variable (fraction survival) because it was a proportion and thus bounded between 0 and 1 (Warton and Hui 2011). This

ensured predictions cannot exceed possible values (e.g. negative survival), and normalized residual error. We generated confidence intervals for parameters and predictions using Monte Carlo methods. For both the lab and field parameterizations we generated 1000 randomized datasets by adding random scatter to each logit transformed observation from a Gaussian distribution with a mean of zero and a standard deviation equal to the standard deviation of residuals of the least-squares model fit to the data. We used a distribution of likely parameter values by fitting the models to these randomized data sets.

## RESULTS

### *Testing the lab-derived model*

For the laboratory data, the phenomenological model captured much of the variation in survival through the embryonic period as a function of temperature (Figure 1;  $R^2=98.28$ ). The least-squares estimate of  $T_{crit}$  and  $b_T$  were  $15.27^\circ\text{C}$  and  $0.028\text{ }^\circ\text{C}^{-1}d^{-1}$ . When applied to the field, the laboratory-parameterized model predicted almost no temperature dependent mortality in the Sacramento River from 1996-2015 (Figure 2). No temperature dependent mortality was predicted in any year, with the exception of 2014 when temperatures reached the highest levels over the 20-year period, and the model predicted temperature dependent mortality of 2%. Because, effectively no temperature-dependent mortality was predicted, the model explained virtually no additional variation in egg-to-fry survival in the field compared to a null model assuming no temperature-dependent mortality ( $r^2 = 0.018$ ). Similar results were found when the null and lab model included a density dependence term (null model with density-dependent background survival  $r^2 = 0.0218$  vs. lab-parameterized thermal tolerance model with density-dependent background survival  $r^2 = 0.0409$ ).

The two most likely explanations for the lab-derived model of thermal tolerance being a poor predictor of annual variation in survival are 1) survival was primarily driven by factors other than temperature, or 2) the thermal tolerance in the field differs from thermal tolerance in the lab. To distinguish between these two hypotheses we repeated our analysis of the field data using  $T_{crit}$  and  $b_T$  as free parameters rather than assuming their lab-derived estimates are applicable to field conditions.

In contrast to the lab parameterization, fitting the model to field data revealed strong evidence of temperature-dependent mortality (Table 1; Figure 2). Most notably, in 2014 and 2015 when temperatures reached the highest levels over the 20 year period, the field-derived model estimated 76% and 86% temperature-dependent embryo mortality rates. The field-parameterized temperature-dependent mortality model vastly outperformed null model ( $\Delta AIC=15.65$ ) and lab model ( $\Delta AIC=15.31$ ) when assuming constant background mortality ( $r^2=0.664$ ). When density-dependent background survival was included, the field-derived model performed even better ( $r^2=0.766$ ) than the null ( $\Delta AIC=22.12$ ) and lab models ( $\Delta AIC=21.76$ ). In the field-parameterized model without density-dependent background survival, the background survival probability was ~28%. When density-dependent term was included, the background survival ranged from roughly ~34% at the lowest female spawner densities observed to ~20% at the highest spawner densities observed ( $\mu_0=0.347$ ;  $\mu_1=1.88e-5$ ; Figure S1).

The differences in survival predicted by the lab and field parameterized models were driven primarily by a ~3°C reduction in  $T_{crit}$  in the field, 12.07°C (95% CI 10.83-13.82) compared to the lab 15.27°C (95% CI 14.80-16.14). Estimates of  $b_T$  were similar between field (0.024, 95% CI 0.0093-8.53) and lab (0.028, 95% CI 0.020-0.042) parameterizations. Due to covariation between  $T_{crit}$  and  $b_T$  in the Monte Carlo analysis, the region of likely parameter space



is much smaller than the individual confidence intervals would suggest (Figure S2). In general most likely parameter sets for the field corresponded to  $T_{crit}$  values in the range of ~11-12.5°C and  $b_T$  values in the same range at the  $b_T$  value estimated from laboratory data. A second, but smaller group (~10%) of Monte Carlo parameter sets had  $T_{crit}$  values around 13.5-14°C and extremely high values of  $b_T$ . These parameter sets corresponded with scenario where embryos are unaffected by temperature up to a relatively high temperature, but exceeding this temperature by small amounts and for short duration results in near complete mortality. Estimates of thermal tolerance parameters in the field were not affected by the inclusion of the density dependent term in the background survival rate ( $T_{crit}$  12.07°C vs. 12.12°C and  $b_T$  0.024 vs. 0.023 in parameterizations with and without a density dependent term in the background survival rate).

#### *Accounting for the discrepancy between lab and field-derived thermal tolerance*

A growing body of experimental and observational studies point to oxygen limitation as a general mechanism setting the thermal tolerance of aquatic ectotherms (Pörtner and Knust 2007, Eliason et al. 2012, Foster et al. 2012; Deutsch et al. 2015). Because developing embryos lack circulatory and ventilation systems, flow velocity and dissolved oxygen strongly influence the oxygen supply rate. In the laboratory environments, Chinook embryos are typically allowed to develop in highly oxygenated, fast flowing water ~0.15 cm/s (USFWS 1999, Beachum and Murray 1989; Jenson and Groot 1991), while in nature, embryos are embedded in gravel redds where flow velocities are lower ~0.04 cm/s (Zimmermann and Lapointe 2005). We therefore developed a biophysical model of oxygen supply and demand for embryos to evaluate whether this mechanism can account for differences in observed thermal tolerances in the lab and field.

Like all obligate aerobes, the supply of oxygen to developing embryos must be sufficient to meet the metabolic demand for oxygen. For a spherical embryo, the supply of oxygen ( $J$ ) to

the developing embryo can be calculated from mass-transfer theory (Daykin 1965, Kranenbarg et al. 2000):

$$J = 4\pi R^2(P_s - P_i)k_e \quad \text{eq.6}$$

where  $R$  is the radius of the sphere,  $P_s$  and  $P_i$  are the oxygen partial pressures (Torr) at the sphere surface and inside the embryo, and  $k_e$  ( $\mu\text{gO}_2/[\text{cm}^2 \text{ s Torr}]$ ) is the mass-transfer coefficient for oxygen transfer to the embryo. Oxygen consumption by the embryo creates an area of local oxygen depletion such that the oxygen concentration at the sphere surface is less than the ambient oxygen concentration  $P_e$ :

$$P_s = P_e - \frac{N\delta}{4\pi R^2 k_w} \quad \text{eq.7}$$

where  $N$  ( $\mu\text{gO}_2/\text{s}$ ) is the oxygen consumption rate of the embryo,  $\delta$  ( $\text{Torr}/[\mu\text{gO}_2/\text{cm}^3]$ ) is a conversion factor from oxygen concentration to pressure, and  $k_w$  ( $\text{cm}/\text{s}$ ) is the mass transfer coefficient of oxygen in water. The mass-transfer coefficient for oxygen in water depends on the combined influence of convective and diffusive transport processes in the water surrounding the developing embryo. In flowing water, a velocity boundary layer forms around the spherical embryo; at the embryo's surface, velocity is zero and it approaches its asymptotic value with increasing distance away from the sphere. Because diffusion is relatively slow in water, a solute boundary forms within the velocity boundary layer. At the egg's surface, oxygen is transported entirely by diffusion and with increasing distance away from the egg convection plays an increasing larger role in oxygen transfer. The combined effect of these processes on oxygen transport from the surrounding water can be estimated via a non-dimensionalization of the Navier-Stokes equation (Daykin 1965, Kranenbarg et al. 2000):

$$k_w = Sh D/2R \quad \text{eq.8}$$

where  $D$  ( $\text{cm}^2/\text{s}$ ) is the diffusion coefficient for oxygen in water and  $Sh$ , is the dimensionless Sherwood number reflecting the ratio of total mass transfer to diffusive mass transfer. For a given geometry,  $Sh$  can be estimated from semi-empirical functions of two other dimensionless numbers: the Reynolds number,  $Re=2RU/\mu$  a ratio of inertial to viscous forces, where  $U$  and  $\mu$  are the velocity ( $\text{cm}/\text{s}$ ) and kinematic viscosity ( $\text{cm}^2/\text{s}$ ) of the surrounding water respectively, and the Schmidt number  $Sc= \mu/D$  a ratio of viscosity and mass diffusivity. For mass transfer to a sphere in flow, the semi-empirical relationship for the Sherwood number is (Daykin 1965):

$$Sh = 2 + 0.8Re^{1/2}Sc^{1/3} \text{ eq.9}$$

Combining eq.6-9 gives oxygen supply to the embryo as a function of its size, its metabolic demand for oxygen, and the velocity and oxygen tension of the surrounding water:

$$J = 4\pi R^2 k_e \left( P_e - P_i - \frac{N\delta}{2DR\pi \left( 2 + 0.8 \left( \frac{\mu}{D} \right)^{1/3} \left( \frac{2RU}{\mu} \right)^{1/2} \right)} \right) \text{ eq.10}$$

At steady state, oxygen demand and supply must balance ( $J=N$ ). When demand for oxygen is low, there is only a small reduction in internal oxygen tension. As demand for oxygen increases,  $P_i$  drops, increasing the concentration gradient until supply again matches demand. Eventually, with increasing demand,  $P_i$  will drop to a level that limits aerobic metabolism,  $P_i^*$ . At this critical point, metabolism switches from being demand driven to being supply constrained. Solving Eq. 10 for the velocity of the surrounding water yields:

$$U_{crit} = \frac{\mu \left( \frac{5N\delta R k_e}{2D(4\pi R^2 k_e (P_e - P_i^*) - N\delta)} + \frac{5}{2} \right)^2}{2R \left( \frac{\mu}{D} \right)^{2/3}} \text{ eq.11}$$

where  $U_{crit}$  is the velocity below which oxygen supply to the embryo is not sufficient to meet demand.

$D$ ,  $\mu$ , and  $\delta$  are well-established physical temperature-dependent parameters (supplementary material, refs). The remaining two supply parameters,  $P_i^*$  and  $k_e$  have been estimated empirically for the embryos of Chinook and other species (Rombough 1989). In general,  $k_e$  was fairly constant among species with markedly different egg capsule properties (Rombough 1989). Because the estimates of  $k_e$  by Rombough (1989) did not explicitly account for the depletion of oxygen at the egg surface, the estimate of  $k_e$  is biased lower than its true value. We recalculated  $k_e$  by accounting for boundary layer effects using eq.7 (supplementary material).

Like most ectotherms, the metabolic demand for oxygen in developing Chinook embryos increases exponentially with temperature (Rombough 1994). Furthermore, as Chinook embryos grow, their demand for oxygen increases in proportion to their live tissue mass. We therefore fit a model for oxygen demand as a function of tissue mass,  $M$  (g), and temperature,  $T$  to data from Rombough (1994):  $N = b_0 M \exp(b_1 T)$ , where  $b_0 = 81.8 \mu\text{gO}_2/\text{g/h}$  and  $b_1 = 0.0945$  ( $R^2=0.95$ ). Eq. 11 predicts that embryos are most vulnerable to oxygen limitation when total oxygen demand,  $N$ , is highest, which will occur right before hatching. We therefore evaluated the oxygen limitation temperature, above which oxygen supply is not sufficient to meet demand for Chinook embryos immediately before hatching (0.05mg).

In general, the temperature at which oxygen becomes limiting is strongly dependent on flow velocity (Figure 3). At the high flow velocities typical for lab experiments ( $> 1\text{mm/s}$ ) the oxygen limitation temperature approaches its asymptotic value where the solute boundary layer becomes infinitely thin, and oxygen supply is constrained only by mass transfer through and

within the sphere. At flows below 1mm/s the thickness of the boundary layer expands rapidly with decreasing flow velocity, reducing the rate of oxygen supply. Consequently, the oxygen limitation temperature drops rapidly with decreasing flow below 1mm/s such that at flow velocities typically observed within gravel redds result in thermal tolerance 2-5°C lower than in the lab, consistent with the discrepancy in thermal tolerance we observed in between lab and field data in our statistical analysis (Figure 3). Not only were the relative differences in thermal tolerance between lab and field well accounted for by the physics of flow, but also the absolute thermal tolerances predicted in the lab and field regimes corresponded closely with the values estimated from our statistical analysis. This supports our hypothesis that oxygen supply and demand is the mechanism driving thermal tolerance of Chinook embryos, and consequently that thermal tolerance is not fixed but is highly dependent on flow.

Among oviparous aquatic embryos, Chinook embryos are outliers with respect to their size, and thus may be more vulnerable to oxygen limitation due to their high surface area to volume ratios. Therefore we addressed whether oxygen limitation broadly underlies the thermal tolerance of developing embryos, or if it is only relevant for the few species with larger egg sizes. We used eq.11 to predict the oxygen limitation temperatures of embryos, where the upper thermal threshold for a species is determined by its embryonic characteristics,  $R$ ,  $N$ ,  $k_e$  and  $P_i^*$ , and environmental characteristic  $P_e$  and  $U$ . Given the little species-specific variation in  $P_i^*$  and  $k_e$  observed among species in Rombough (1989) we fixed these values to those used for Chinook salmon. To determine  $N$ , we compiled respiration data for developing embryos using the last observed metabolic rate before hatching. We fit an allometric relationship between embryo radius and temperature corrected metabolic rate before hatching (supplementary material), where  $N_0 = a_1 R^{a_2}$  ( $a_1 = 200.8 \mu\text{gO}_2/\text{embryo}/\text{h}$  and  $a_2 = 3.03$ ,  $R^2 = 0.94$ ) and  $N = N_0 e^{dT}$ . The allometric

relationship explained most of the variance in embryonic oxygen demand, however given the vast differences in sizes, any particular observation could vary by a factor of 2-3.

Using the parameter values specified above, we compared the predicted oxygen limitation temperatures to observed development temperatures of ~180 fish species compiled from three sources (Ware 1975, Pauley and 1989, and the STOREFISH database [Teletchea et al. 2007; 2009]). The values used reflect temperatures in which the embryos have been observed to have developed, but not necessarily their upper limit. Our simple model, based on the physics of oxygen diffusion captured several salient patterns of variation: 1) observed developmental temperatures of species were negatively related their radius, 2) for a size, species that undergo embryonic development in high flow environments (e.g. spawn in rivers or exhibit parental nest fanning) tended to have a higher thermal tolerance, 3) the observed developmental temperatures of species were clustered around the predicted thermal limits for a given egg size and developmental flow regime (Figure 5).

## **DISCUSSION**

Our analysis underscores the potential pitfalls of extrapolating phenomenological models of thermal stress from the lab to the field. Our lab-parameterized model of thermal tolerance failed to predict the substantial temperature-dependent mortality revealed by our field analysis. In the case of Sacramento River Chinook salmon, field-derived estimates of thermal tolerance can be used to re-evaluate temperature management actions to protect salmon eggs. However, for most species the necessary field survival data are not available. For these species it is necessary to understand the mechanisms that underlie thermal tolerance to translate measures in laboratory settings to variable environmental conditions.

We found strong support for the role of oxygen limitation as the mechanism underlying the thermal tolerance of fish embryos. While the physics of mass-transfer to a sphere have been worked out for a half a century (Daykin 1965), the theory has not been applied to predict the thermal tolerance of embryos. The model is elegantly simple, requiring only four biological parameters - two to specify temperature dependent oxygen demand, as well as the critical oxygen tension and mass transfer coefficient of the embryo – to predict thermal tolerance as a function of egg size, dissolved oxygen, and flow velocity. All four of these parameters can be measured using simple respirometry techniques (Rombough 1989). Furthermore, the parameters vary little across species such that we were able to predict thermal tolerance from egg size alone. Our model can explain 94% of the variation in oxygen demand using fixed oxygen demand parameters. The remaining two parameters,  $P_i^*$  and  $k_e$ , Rombough (1989) were relatively constant across size for different species of salmonids. Although, further work is needed to evaluate these parameters for a wider subset of species, we were able capture multiple patterns related to the thermal tolerance of embryos by fixing these parameters to the values for Chinook. Our results add to a growing body of empirical evidence of the importance of oxygen limitation in determining the thermal tolerance of aquatic species. More importantly, 97% of the worlds fish species are oviparous, and our model allows for testable quantitative predictions for how thermal tolerance will scale with embryo size and environmental conditions for this critical developmental stage.

The physics of diffusion set an upper limit on the metabolic rate an embryo of a given size can sustain. Our analysis of observed developmental temperatures suggests that the metabolic demand of most embryos frequently approach this limit (Figure 4). This is likely due to the significant tradeoffs required to increase thermal resilience. Species could increase  $k_e$  (the

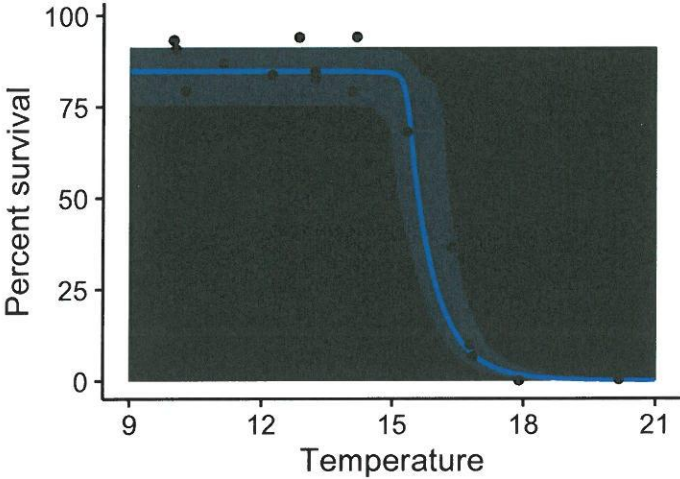
mass-transfer coefficient for oxygen transfer to the embryo) or decrease  $P_i^*$  (oxygen partial pressure at which aerobic metabolism is limited), however the consistency of these parameters across species suggest their limited capacity for change to improve oxygen supply. For example,  $k_e$  has likely been selected to be as high as possible while still maintaining enough structural integrity.  $P_i^*$  is obviously constrained to positive values and dropping  $P_i^*$  from ~40-50 Torr to 0 would only boost thermal tolerance by a 3-4°C. Otherwise, fish only have two options to increase embryonic thermal tolerance. They could produce small eggs, resulting in smaller, less developed juveniles. Or, they could produce eggs with a lower volume-specific metabolic rate, resulting in longer development time during which they are highly vulnerable to predation (McGurk 1986). Considering the drawbacks associated with either option, it is perhaps not surprising that when thermal stress is relaxed in cooler waters, species have responded by producing larger eggs (Ware 1975, Pauly and Pullin 1988). Moreover, many species with embryonic stages occurring in environments with high flow velocities (such as rivers), take advantage of the improved capacity for oxygen supply by producing larger eggs. In other cases, species produce larger eggs in warm environments than otherwise be viable and compensate by paying enormous energetic costs by fanning their eggs.



Table 1. Comparison of phenomenological models performance at predicting inter-annual variation in egg-to-fry survival of winter run Chinook in the Sacramento River.

Model	df	SSQ	$r^2$	AIC	$\Delta$ AIC
Field model + density dep.	4	2.171	0.771	-28.071	0
Field model	3	3.180	0.664	-23.203	-4.868
Lab model + density dep.	2	9.085	0.041	-6.307	-21.764
null + density dep.	2	9.267	0.022	-5.951	-22.120
Lab model	1	9.298	0.018	-7.890	-20.181
Null	1	9.473		-7.555	-20.516

**Figure 1.** Fit of the phenomenological temperature-dependent mortality to laboratory data on survival through the embryonic period as a function of temperature (data from Combs and Burrows 1957; USFWS 1999; Jensen and Groot 1991). Mean (solid line) and 95% CI (shaded region) of 1000 Monte Carlo parameter values.



**Figure 2.** Model predictions for egg-to-fry survival and temperature-dependent mortality of Sacramento River Winter run Chinook using thermal tolerance parameters from laboratory (left column) or field data (right column). Observed vs. predicted egg-to fry survival in the lab and field-parameterized models (A and B). Observed (black points) and predicted (red points, dashed lines) egg-to-fry survival across years (C and D). Lab and field-parameterized model predictions for the percent of population lost in years due to temperature-dependent mortality (E and F), with 95% CI from the Monte Carlo analysis (error bars).

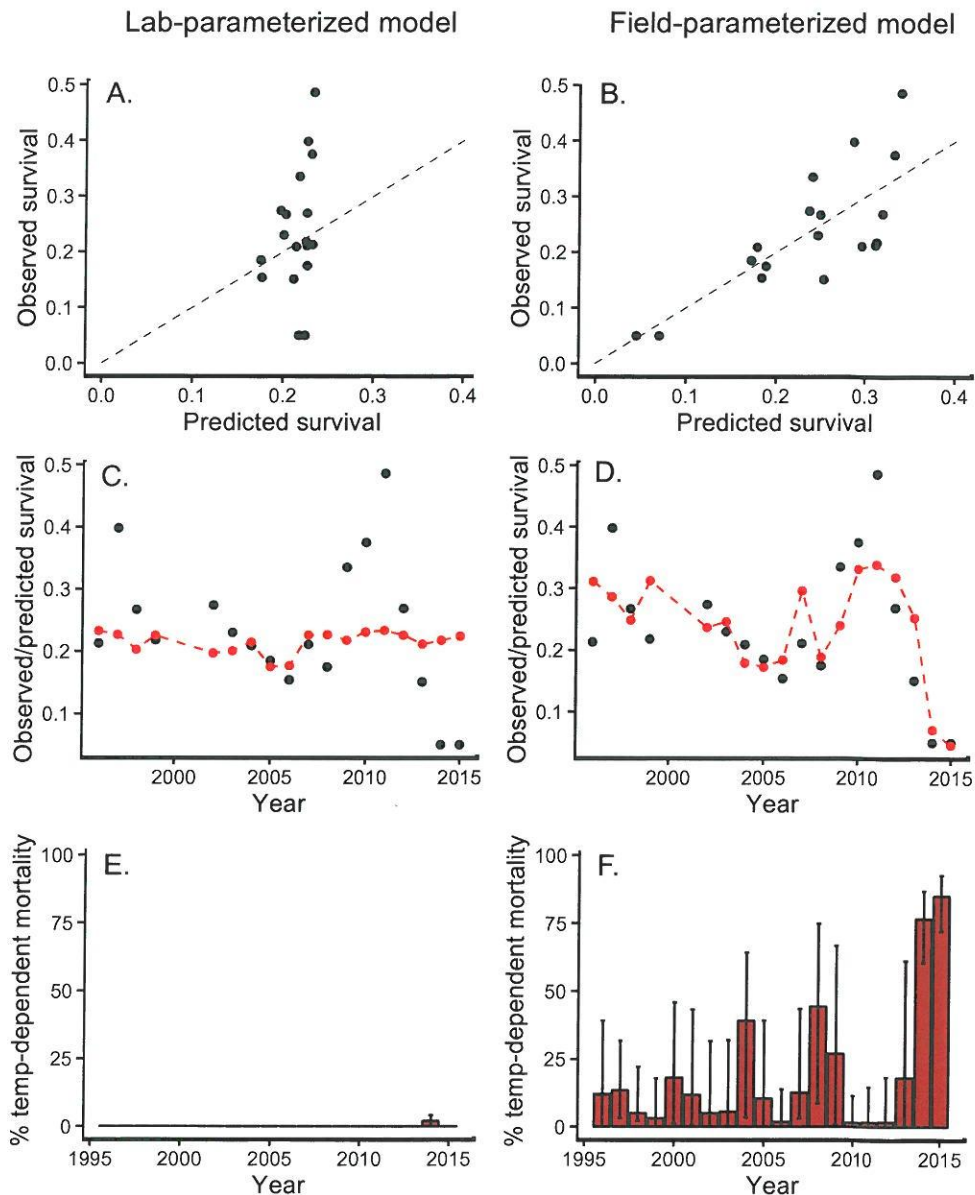


**Figure 3.** Comparison of statistically (left) and mechanistically (right) determined thermal tolerances in lab (blue) and field (red) contexts. Distribution of 1000 Monte Carlo parameter estimates (left panel) for  $T_{crit}$  when fit using lab (blue) and field (red) data. The mechanistically determined oxygen limitation temperature (the temperature above which oxygen supply is insufficient to meet demand) for a Chinook embryo at a size near hatching (0.05mg) as a function of the velocity of the surrounding water at 100% oxygen saturation (right panel). Ranges of flow velocities typically found in lab (shaded blue region, from USFWS 1999, Beachum and Murray 1989; Jenson and Groot 1991) and field (shaded red region, from Zimmerman and LaPointe 2005) contexts respectively.

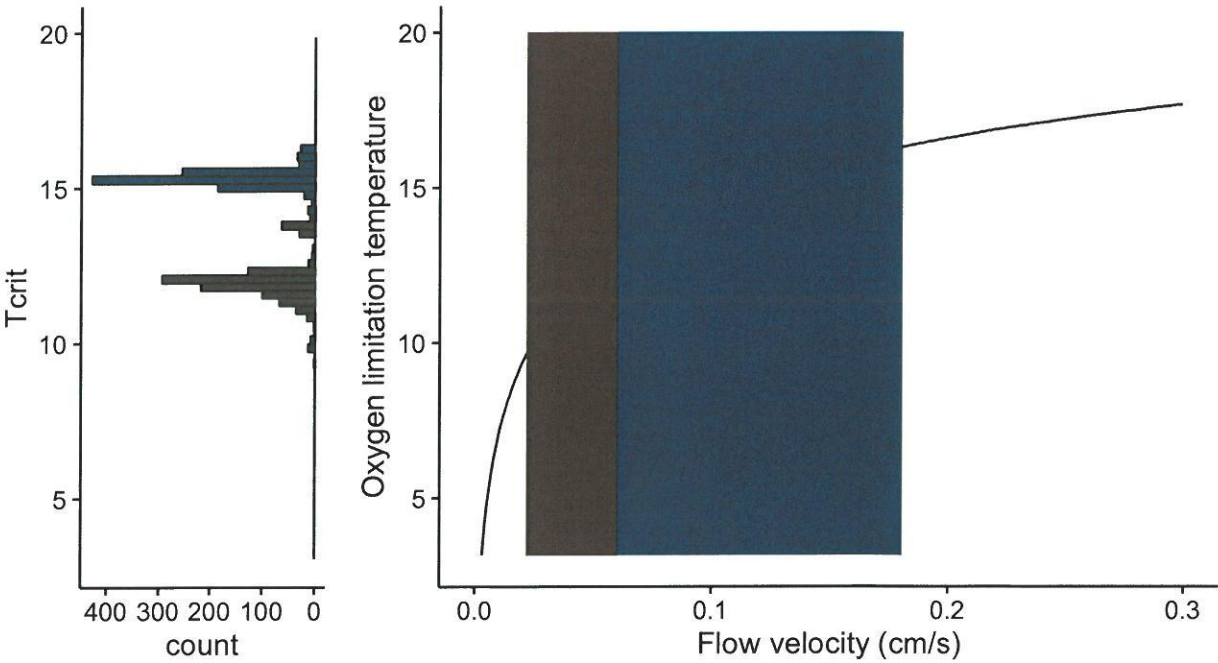
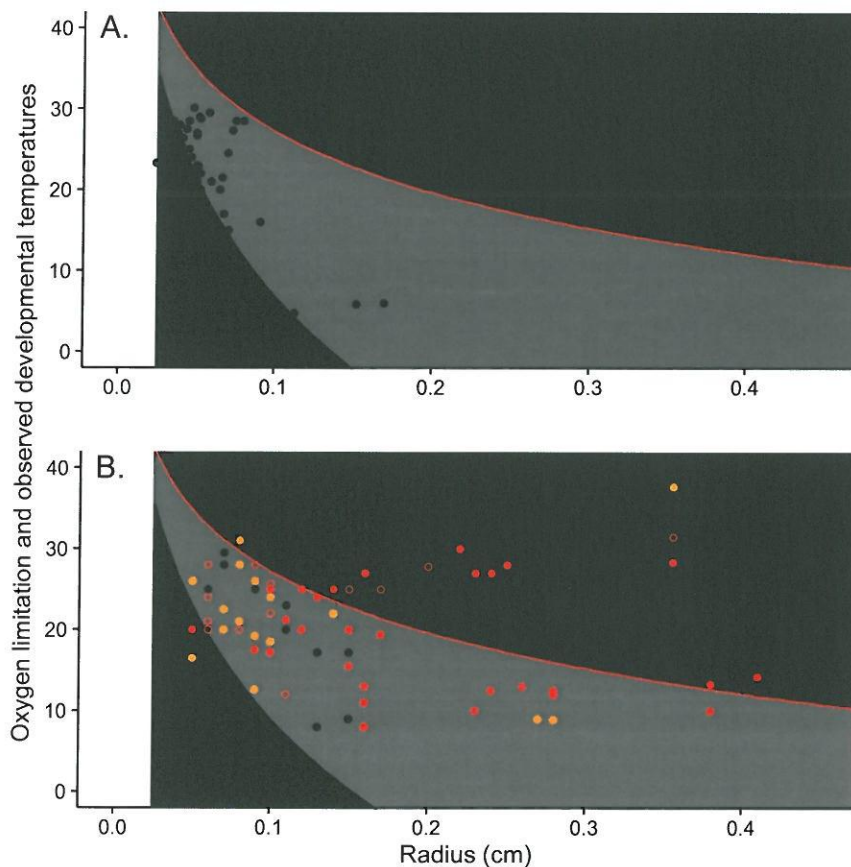


**Figure 4.** Predictions of oxygen limitation temperature as a function of egg size (radius) and flow regime. The black line is the oxygen limitation temperature at which oxygen becomes limiting in stagnant water and red is the oxygen limitation temperature in infinitely fast flowing water. The top panel compares predicted oxygen limitation temperatures with observed developmental temperatures of pelagic marine embryos (Ware 1975; and Pauly and Pullin 1988). Bottom panel are freshwater spawning species separated by groups (river spawners, non-river spawners, mixed (spawns both in river and non-river habitats) spawners, and parental fanners) from the STOREFISH database (Teletchea et al. 2007; 2009). Observed development temperatures do not necessarily reflect the upper thermal limits of species. When multiple developmental or egg sizes were recorded for a species we used the maximum non-lethal developmental temperature recorded and the mean egg size.



## Supplementary figures

**Figure S1.** Influence of female spawner density on background survival rate. Panel A shows the time series of the number of returning female spawners. Panel B shows the relationship between annual egg-to-fry (ETF) survival of winter-run Chinook and female spawner density. Panel C shows this seem relationship but with observed ETF corrected to exclude mortality due to temperature (corrected ETF = Observed ETF / (1 – fractional population loss due to temperature alone)). The red line in panels B and C is the predicted background survival rate from the field-parameterized model.

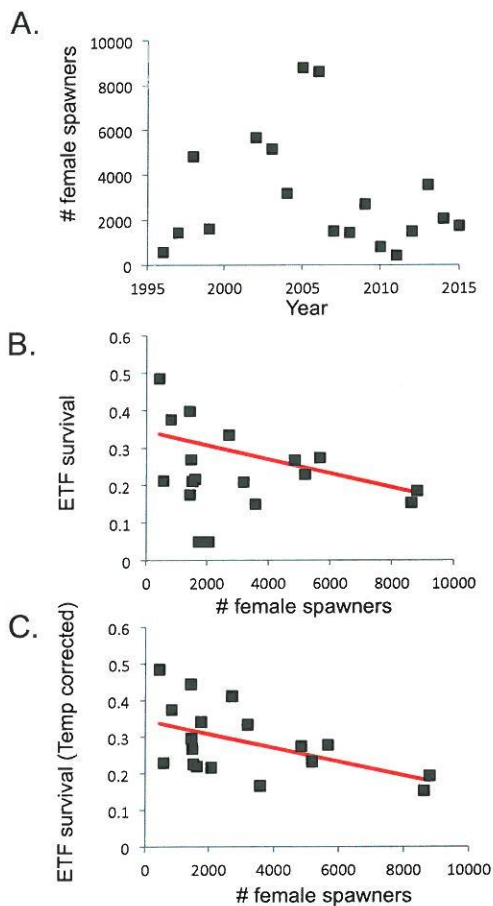




**Figure S2.** Comparison of field (red) and lab (blue) estimates of thermal tolerance parameters.

The top and right histograms show distribution of likely parameter estimates for  $T_{crit}$  and  $bT$  from the Monte Carlo analysis of 1000 randomized datasets. The scatter plot shows the covariance between the thermal tolerance parameter estimates in the lab and field parameterizations.

